Journal of Steel Structures & Construction
ISSN: 2472-0437
Wang and Lui, J Steel Struct Constr 2016, 2:2
DOI: 10.4172/2472-0437.1000123
Review Article
Open Access

Behavior of High Strength Steels under and After High Temperature Exposure: A Review

F Wang and E M Lui*

Department of Civil and Environmental Engineering, Syracuse University, Syracuse, NY 13244-1240, USA

Abstract

Fire-resistant and high temperature behavior of high strength steels (HSS) for structural engineering applications has become an important research topic in recent years. In this paper, a succinct review of HSS behavior under and after high temperature exposure is provided. The review addresses the following aspects of HSS: (1) their mechanical properties under and after fire exposure, (2) residual stress in welded HSS sections, and (3) high temperature performance of HSS columns. Recent studies have demonstrated that different grades of HSS can exhibit noticeable differences in their mechanical properties under and after fire exposure, and different cooling methods could have an effect on the post-fire mechanical properties of HSS. Because current design standards for steel structures under elevated temperature were developed based on mild steel, care must be exercised when applying these standards to HSS as they are not necessarily applicable.

Keywords: High strength steel; Mechanical properties; Elevated temperature; Post-fire; Residual stress

Introduction

From 1960s to 1990s, ASTM A36 (with a nominal yield strength of 36 ksi or 248 MPa) was the predominant structural steel used for building construction while high-strength low-alloy and quenched and tempered alloy steels (with nominal yield strength that varies from 50 to 100 ksi or 248 to 690 MPa) were used as alternatives for special applications. In the USA, ASTM A992 adopted in 1998 is currently the most commonly used steel for W-shaped sections [1]. High strength steels (HSS), with a nominal yield strength no less than 67 ksi or 460 MPa, is permitted for use under special circumstances, such as for high-rise buildings and long-span bridges. When compared with conventional steel, structures built using HSS offer advantages in increased strength and reduced weight, which could lead to economy in construction. As a result, research on the behavior and application of HSS has become an important topic in the structural engineering community [2-5].

Historical events have clearly demonstrated that fire hazard is a major threat to the structural integrity of a structure throughout its service life. Although most steel structures can withstand a fire or exhibit no visible structural damage after fire exposure, post-fire elements may experience residual stress change and deformations during cooling. Research on HSS behavior both under and after fire exposure has been conducted by various researchers to evaluate the fire-resistance and residual strength of HSS structures. This paper presents a concise review on the behavior of HSS under and after high temperature exposure, including mechanical properties of different types of HSS, residual stress induced in welded HSS sections, and high temperature performance of HSS columns [6].

Steel Grade Representation

Generally, different countries have different notations for designating steel grade. Based on Chinese Standard GB/T 1591-2008, 420 MPa steel is designated as Q420, where the letter Q is the Chinese phonetic alphabet of the word "Qu" meaning steel yield strength and the number 420 is the nominal yield strength in MPa. In Europe, according to EN10025-2004, 420 MPa steel is designated as S420, where S represents structural steel and 420 is the nominal yield strength in MPa [7].

Behavior of HSS under Elevated Temperature

After the 9/11 attack on the twin towers in New York City, fire resistance of steel structures has become an important research topic in the structural engineering community. Research on the mechanical properties of mild and HSS steels at elevated temperatures has been carried out by a number of researchers. There are two common methods that can be used to test the mechanical properties of steel under elevated temperatures, steady-state and transient-state. In a steady-state test, the test specimen is first heated to a predefined temperature [8]. A tensile load is then applied to the specimen while the temperature is held constant. In a transient-state test, the test specimen is first pre-loaded to a predetermined force. It is then heated slowly to the target temperature. Steady-state tests are more often conducted because they can be performed over a shorter period of time [9-12]. However, transient-state tests tend to produce more realistic results since the effects of creep and relaxation can be accounted for.

A summary of tests for different types of HSS under elevated temperature is given in Table 1.

The letter M designates thermomechanical rolled steel, N designates normalized rolled steel, Q designates quenched and tempering, L designates low notch toughness testing temperature, and RQT designates reheated, quenched and tempered. BISPLATE 80 is fabricated by an Australian company BISALLOY®, which is somewhat equivalent to ASTM A514 and S690. 20MnTiB is a type of HSS with a yield strength exceeding 940 MPa.

The mechanical properties (elastic modulus, yield strength, tensile strength) of HSS under elevated temperatures can be determined

***Corresponding author:** Department of Civil and Environmental Engineering, Syracuse University, Syracuse, NY 13244-1240, USA, Tel: (315)443-3394; E-mail: emlui@syr.edu

Received December 14, 2016; **Accepted** December 24, 2016; **Published** December 30, 2016

Citation: Wang F, Lui EM (2016) Behavior of High Strength Steels under and After High Temperature Exposure: A Review. J Steel Struct Constr 2: 123. doi: 10.4172/2472-0437.1000123

from the stress-strain curves. Since these properties usually degrade as temperature rises, reduction factors are often introduced to represent the change in mechanical properties with temperature.

Elastic Modulus

Tables 2 and 3 provide a summary of reduction factors for elastic modulus obtained for different types of HSS.

According to Tables 2 and 3, the reduction in elastic modulus varies depending on the type of HSS and tests used. Also, different fabrication method and alloy composition will lead to different results. For design purpose, Wang et al. [3] and Qiang et al. [13] performed regression analysis on the test results for Q460 and S460N steels and developed equations that can be used to determine E_T, the elastic modulus at temperature T (°C), given E_{20}, the elastic modulus at 20°C (room temperature), and T. The equations are given in Table 4. For purpose of comparison, the elastic modulus reduction factors for four HHS (Q460, S460N, S690QL based on steady-state test and BISPLATE80) and those recommended by the American Institute of Steel Construction developed based on tests of mild steel are plotted in Figure 1. As can be seen, they do differ over the range of temperature shown, although the reduction factors for S460N and mild steel are somewhat comparable.

Yield Strength

Study on the yield strength of HSS at elevated temperatures has also been conducted. Since most HSS show no obvious yield plateau, the yield strength is determined at an offset of 0.2% strain as per ASTM E21-09 (Table 4).

In current design standards, the reduction factors for yield strength recommended by the European Steel Design Code (EC3) are based on a strain level of 2.0%, and in the British Standard for Steel Work Design (BS5950) different reduction factors are given based on three strain levels of 0.5%, 1.5% and 2.0%. In American Steel Design Specifications (AISC) and the Australian Standard for Steel Structures Design (AS 4100), no specific strain level is mentioned, but a 0.2% yield strength is assumed. The 0.2% yield strength is the intersection point of the stress-strain curve and a line drawn parallel to the proportional line at a strain value of 0.2%. On the other hand, the yield strength at 0.5, 1.5 and 2.0% strain levels are determined as the intersection point of the stress-strain curve and a vertical line drawn at the specified strain [15].

Tables 5 and 6 summarize the reduction factors for yield strength obtained for different types of HSS.

Because of the blue brittleness effect in the steady-state test of Q460 steel, a small increase in strength and a decrease in ductility were observed. This phenomenon occurred in 200~450°C and resulted in a "reduction factor" larger than 1 at 300°C [3].

Steel type	Test method	Temperature range (°C)	Heating rate (°C/min)	Control parameter
Q420 [2]	Steady	20~600	-	Load: 0.1 kN/s
	Transient	30~550	48~54	-
Q460 [3, 4]	Steady	20~800	-	Load: 0.5 kN/s
S420M [5]	Transient	20~700	10	-
S460 [6]	Transient	20~950	20	-
S460M [7-10]	Steady	200~800	-	Strain: 0.002~0.005/min
S460N [7-10]	Transient		3, 6, 10, 20, 30	-
S460N [11-13]	Steady	20~700	-	Strain: 0.005/min
	Transient		10	-
BISPLATE80 [14]	Steady	22~940	-	Strain: 0.006/min
	Transient	22~660	-	-
S690QL [15]	Steady	20~700	-	Strain: 0.005/min
	Transient		10	-
RQT-S690 [16]	Steady	25~800	-	Strain: 0.003/min
20 Mn-TiB [17]	Steady	20~700	-	Strain: 0.1/min

Table 1: Summary of tests on HSS at elevated temperature.

T (°C)	Q460 [3]	S460N [9]	S460M [9]	S460N [11-13]		S690QL [15]		RQT- S690 [16]
				Steady	Transient	Steady	Transient	
20	1	-	-	1	1	1	1	1 (25°C)
100	0.983	1	1	0.985	0.989	1	0.982	1.01
200	0.960	0.885	0.976	0.881	0.870	0.875	0.869	1.02
250	0.945	0.838	0.964	0.840	0.831	0.857	0.857	0.99
300	0.928	0.791	0.952	0.799	0.792	0.839	0.841	0.96
350	0.911	0.730	0.920	0.712	0.702	0.807	0.781	0.99
400	0.885	0.668	0.887	0.669	0.666	0.775	0.736	1.01
450	0.862	0.575	0.796	0.578	0.585	0.730	0.692	0.91
500	0.836	0.481	0.704	0.509	0.482	0.685	0.647	0.77
550	0.809	0.392	0.555	0.374	0.359	0.546	0.537	0.72
600	0.764	0.302	0.406	0.291	0.272	0.372	0.370	0.66
650	0.636	0.219	0.305	0.248	0.222	0.257	0.204	0.38
700	0.480	0.135	0.204	0.153	0.132	0.141	0.099	0.34
800	-	0.049	0.105	-	-	-	-	0.29
900	-	0.017	0.038	-	-	-	-	-

Table 2: Summary of reduction factor for elastic modulus.

T (°C)	BISPLATE80 [14]	
	Steady	Transient
22	1	1
60	1.04	0.92
120	1.01	0.89
150	1.04	0.86
180	1.02	0.82
240	0.98	0.77
300	1.00	0.74
360	0.95	0.68
410	0.92	0.64
460	0.94	0.61
540	0.87	0.6
600	0.73	0.44
660	0.73	0.32
720	0.51	-
770	0.49	-
830	0.33	-
940	0.12	-

Table 3: Summary of reduction factor for elastic modulus (Cont'd).

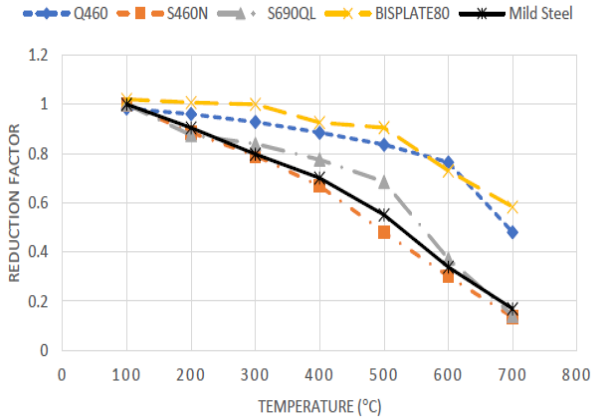

Figure 1: Comparison of reduction factor for elastic modulus.

Using regression analysis, empirical equations that relate f_{yT}, the yield strength of HSS at temperature T (°C), and f_y, the yield strength at 20°C (room temperature) before the HSS is exposed to high temperature, were developed [3,13] and shown in Table 7.

The yield strength reduction factors for four HHS (Q460, S460N, S690QL 0.2% yield strength based on state-state test, and BISPLATE80) are compared in Figure 2 to those recommended by the American Institute of Steel Construction developed based on tests of mild steel. As can be seen, noticeable differences are observed for the different types of steel [16-18].

Tensile (or Ultimate) Strength

When temperature rises, the tensile or ultimate strength of HSS decreases. However, the effect of tensile strength loss is negligible until the temperature rises above 350°C. Reduction factors for tensile strength are summarized in Table 8 and empirical equations that can be used for design are given in Table 9.

In the above Table, f_{uT} is the tensile strength at temperature T (°C) and f_u is the tensile strength at 20°C before the HSS is exposed to high temperature.

In Figure 3, the tensile strength reduction factors for four HHS (Q460, S460N, S690QL based on steady-state test, BISPLATE80) are compared to those recommended by the American Institute of Steel Construction developed based on tests of mild steel. As can be seen, except for Q460, the reduction factors for other HSS are generally lower than those for mild steel when the temperature exceeds 300°C.

Post-fire Behavior of HSS

*****Generally, two methods can be used to conduct cooling tests on steel after exposure to elevated temperature. They are the air-cooling and water-cooling methods. Of the two, the water-cooling method is more realistic. Wang et al. [18] showed that the use of water cooling had a dramatic influence on the post-fire tensile strength and elongation of the test specimens. Table 10 summarizes the post-fire tests on some HSS.

Using regression analysis, Wang et al. [18] proposed empirical equations for determining post-fire mechanical properties of Q460 steel. Depending on the type of cooling used, two sets of equations are proposed. They are shown in Table 11.

Qiang et al. [19,20] pointed out that when the temperature was below 600°C the post-fire mechanical properties loss of S460, S690 and S960 were negligible. Furthermore, all test specimens showed ductile failure with necking and no brittle failure was observed. Empirical equations for post-fire mechanical properties of these HSS were developed and they are summarized in Tables 12-14.

Residual Stress of HSS

Residual stress is developed as a result of uneven cooling of the different parts of the cross-section during the fabrication process. The presence of residual stress could result in early yielding and reduction in stiffness. While residual stress of normal strength hot-rolled and welded steel sections has been widely studied, the same cannot be said for HSS.

Wang et al. [21] studied three welded flame-cut Q460 HSS H-section members with three different width-to-thickness ratios, 3.4, 5 and 7.1. Ban et al. [22] and Yang et al. [23] conducted a similar study with a larger range of width-to-thickness ratios on 460 MPa HSS welded I-shaped members and Q460GJ HSS welded I-shaped members, respectively. The residual stress distribution they obtained was found to be similar to that of mild steel with lower magnitudes and was related to section dimensions. Furthermore, Kim et al. [24] tested 800 MPa HSS welded box-, cruciform- and H-sections, and Li et al. [25] provided information on the magnitude and distribution of residual stresses for box- and H-sections made of Q690 steels.

However, it should be noted that the investigation on the magnitude and distribution of residual stress for post-fire HSS welded section members is rather limited. Wang et al. [26,27] performed residual stress tests on welded Q460 H-sections after fire exposure, shown in Table 15, and found that the magnitude of post-fire residual stress decreased significantly with an increase in temperature.

Behavior of HSS Columns under Elevated Temperature

Valente and Neves [28], Rodrigues et al. [29] and Tan et al. [30] studied the fire resistance of mild steel columns and found that the presence of axial restraint would decrease the critical temperature, which is the temperature at which failure of the member occurs. Wang and Ge [31] conducted a similar research on four Q460 H-shaped columns using two levels of axial constrained stiffness and two levels of axial load ratio. The test results, given in Table 16, show that for a

Steel type	Empirical equation	Temperature range (°C)
Q460 [3]	$E_T / E_{20} = 1.02 - 0.035e^{T/280}$	20 ≤ T ≤ 800
S460N [13]	$E_T / E_{20} = 2.961\times10^{-9}T^3 - 4.317\times10^{-6}T^2 + 3.867\times10^{-4}T + 0.986$	20 ≤ T ≤ 900

Table 4: Empirical equations for elastic modulus of HSS at elevated temperatures.

T (°C)	Q460 [3]	S460N [9]	S460M [9]	S460N [11-13]					RQT- S690 [16]			
				Steady	Transient				Steady			
				2 %	0.2 %	0.5 %	1.5 %	2 %	0.2 %	0.5 %	1.5 %	2 %
20	1	1	1	1	1	1	1	1	1	1	1	1
100	0.88	0.878	0.947	0.987	0.9	0.903	0.952	0.989	0.947	0.874	0.958	0.968
150	0.98	0.901	0.948	0.991	0.902	0.9	0.944	0.975	0.916	0.866	0.957	0.975
200	1.07	0.924	0.949	0.994	0.809	0.821	0.923	0.97	0.884	0.854	0.956	0.982
250	1.11	0.913	0.952	0.998	0.802	0.796	0.909	0.966	0.882	0.803	0.954	0.979
300	1.14	0.901	0.954	1.001	0.78	0.773	0.903	0.962	0.879	0.751	0.952	0.975
350	1.09	0.884	0.956	0.984	0.756	0.741	0.895	0.958	0.837	0.773	0.908	0.913
400	1.03	0.867	0.958	0.949	0.716	0.718	0.883	0.942	0.794	0.794	0.864	0.85
450	1.06	0.769	0.916	0.877	0.665	0.69	0.848	0.899	0.711	0.7	0.76	0.737
500	0.85	0.67	0.874	0.739	0.532	0.635	0.777	0.771	0.628	0.605	0.655	0.624
550	0.74	0.551	0.722	0.559	0.446	0.534	0.644	0.639	0.554	0.438	0.557	0.533
600	0.73	0.432	0.57	0.415	0.364	0.457	0.499	0.495	0.38	0.345	0.382	0.371
650	0.55	0.316	0.445	0.313	0.276	0.318	0.384	0.381	0.24	0.23	0.258	0.252
700	0.36	0.2	0.32	0.187	0.22	0.246	0.287	0.247	0.1	0.114	0.133	0.133
800	0.18	0.071	0.12	-	-	-	-	-	-	-	-	-
900	-	0.034	0.048	-	-	-	-	-	-	-	-	-

Table 5: Summary of reduction factor for yield strength.

T (°C)	S690QL [15]								T (°C)	BISPLATE80 [14]			
	Steady				Transient					Steady			
	0.2%	0.5%	1.5%	2%	0.2%	0.5%	1.5%	2%		0.2%	0.5%	1.5%	2%
20	1	1	1	1	1	1	1	1	22	1	1	1	1
100	0.947	0.874	0.958	0.968	0.985	0.989	0.91	0.923	60	0.95	0.96	0.96	0.96
150	0.916	0.864	0.957	0.975	0.924	0.934	0.873	0.896	120	0.94	0.94	0.96	0.96
200	0.884	0.854	0.956	0.982	0.863	0.878	0.836	0.868	150	0.96	0.95	0.98	0.99
250	0.882	0.803	0.954	0.979	0.858	0.875	0.831	0.861	180	0.92	0.92	0.97	0.97
300	0.879	0.751	0.952	0.975	0.837	0.872	0.826	0.855	240	0.89	0.89	0.99	1
350	0.837	0.773	0.908	0.913	0.803	0.839	0.813	0..839	300	0.89	0.9	0.98	0.99
400	0.794	0.794	0.864	0.85	0.797	0.812	0.786	0.798	410	0.87	0.87	0.94	0.94
450	0.711	0.7	0.76	0.717	0.758	0.763	0.73	0.738	460	0.8	0.81	0.85	0.84
500	0.628	0.605	0.655	0.624	0.627	0.631	0.716	0.716	540	0.75	0.75	0.76	0.74
550	0.554	0.438	0.557	0.533	0.54	0.542	0.554	0.554	600	0.6	0.61	0.56	0.59
600	0.38	0.345	0.382	0.371	0.396	0.397	0.445	0.445	660	0.43	0.44	0.43	0.42
650	0.24	0.23	0.258	0.252	0.295	0.213	0.278	0.278	720	0.21	0.21	0.22	0.22
700	0.1	0.114	0.133	0.133	0.163	0.228	0.203	0.203	770	0.14	0.14	0.15	0.14
800	-	-	-	-	-	-	-	-	830	0.08	0.08	0.08	0.09
900	-	-	-	-	-	-	-	-	940	0.05	0.05	0.05	0.05

Table 6: Summary of reduction factor for yield strength (Cont'd).

given constrained stiffness, the critical temperature decreases when the axial load ratio increases, or for a given axial load ratio, the constrained stiffness needs to be increased to maintain the critical temperature. Using finite element analysis, Ge and Wang [32] compared the inelastic strength of Q460 with Q235 steels shown in Table 17, and demonstrated the beneficial effect of using higher strength steel to counteract the loss of inelastic stability caused by the larger slenderness ratio of HSS.

Wang et al. [33] tested twelve welded H-shaped Q460/Q235 steel stub columns given in Table 18 under axial compression with the objective of studying the local instability behavior at different elevated temperatures. The failure modes of all the specimens were local buckling, which are similar to those under room temperature.

From Table 18, it can be seen that the decrease of buckling strength is occurring at a higher rate than yield strength. This is because inelastic buckling is a function of both yield strength and stiffness. Since both are decreasing with an increasing temperature, their combined effect is manifested in the noticeable reduction in inelastic buckling strength.

Using the finite element software ABAQUS, Chen and Young [34] analyzed several HSS box and I-section columns (Table 19) at elevated temperatures, and concluded that while the current AISC specification conservatively predicted the behavior of HSS columns at elevated

Steel type	Empirical equation	T Range (°C)
Q460 [3]	$f_{yT}/f_y = 1$	20 ≤ T ≤ 450
	$f_{yT}/f_y = 4.32e^{-T/880} - 1.6$	450<T ≤ 800
S460N [13]	$f_{yT}/f_y = 1.001 - 1\times10^{-4}T$	20 ≤ T ≤ 350
	$f_{yT}/f_y = -1.672\times10^{-11}T^4 + 5.135\times10^{-8}T^3 - 5.41\times10^{-5}T^2 + 2.138\times10^{-2}T - 1.835$	350 < T ≤ 900

Table 7: Empirical equations for yield strength of HSS at elevated temperatures.

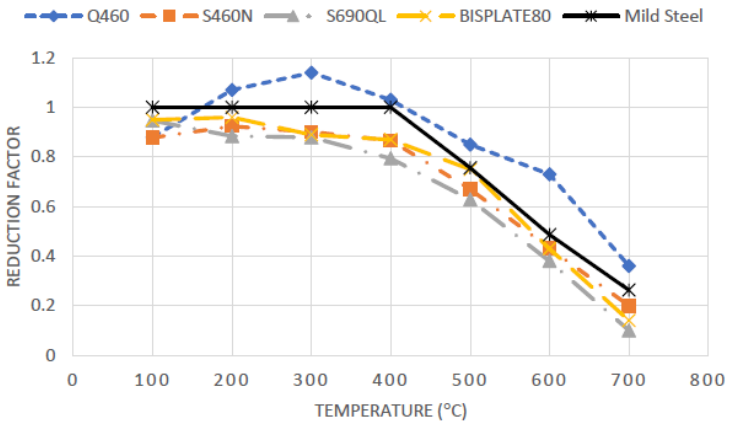

Figure 2: Comparison of reduction factor for yield strength.

T (°C)	Q420 [2]	Q460 [3]	S460N [11-13]		S690QL [15]		RQT- S690 [16]	T (°C)	BISPLATE80 [14]
	Steady	Steady	Steady	Transient	Steady	Transient	Steady		Steady
20	1	1	1	1	1	1	1(25°C)	22	1
100	0.974	0.93	0.945	0.998	0.968	0.923	0.96	60	0.959
150	0.958	0.96	0.957	0.969	0.975	0.896	0.96	120	0.97
200	0.925	0.98	0.969	0.968	0.982	0.868	0.95	150	0.992
250	1.012	1	0.996	0.968	0.979	0.861	0.96	180	0.983
300	1.082	1.02	1.023	0.968	0.975	0.855	0.97	240	0.999
350	1.156	1.03	1.024	0.968	0.913	0.839	0.91	300	0.994
400	1.107	1.03	0.88	0.968	0.85	0.798	0.84	410	0.929
450	0.994	1	0.75	0.897	0.737	0.738	0.64	460	0.819
500	0.828	0.82	0.601	0.693	0.624	0.716	0.5	540	0.732
550	0.668	0.63	0.443	0.556	0.533	0.554	0.35	600	0.588
600	0.431	0.6	0.328	0.421	0.371	0.445	0.19	660	0.421
650	-	0.45	0.249	0.278	0.252	0.278	0.15	720	0.21
700	-	0.29	0.157	0.206	0.133	0.203	0.1	770	0.14
800	-	0.15	-	-	-	-	0.07	830	0.089
900	-	-	-	-	-	-		940	0.051

Table 8: Summary of reduction factor for tensile strength.

Steel Type	Empirical equation	Temp. Range (°C)
S460N [13]	$f_{uT}/f_u = 1 - 1.855\times10^{-5}T$	20 ≤ T ≤ 350
	$f_{uT}/f_u = -7.079\times10^{-11}T^4 + 1.73\times10^{-7}T^3 - 1.526\times10^{-4}T^2 + 5.52\times10^{-2}T - 5.985$	350<T ≤ 900

Table 9: Empirical equations for tensile strength of HSS at elevated temperatures.

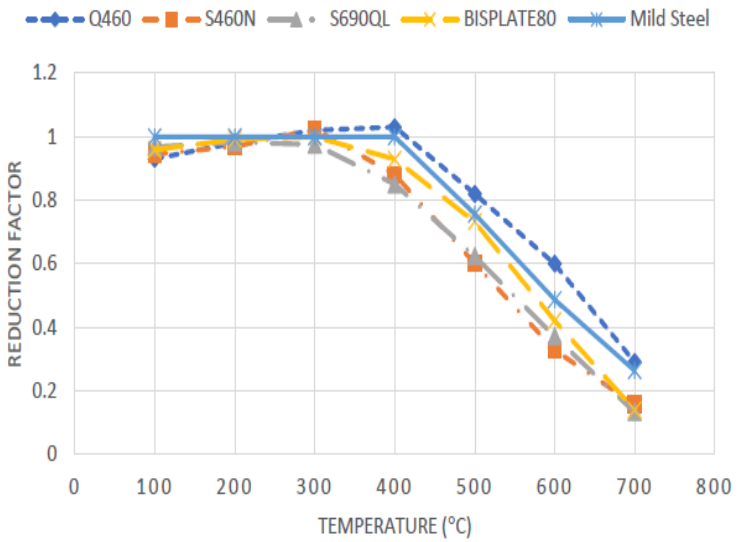

Figure 3: Comparison of reduction factor for tensile strength.

Steel type	Temperature range (°C)	Test method	Heating rate (°C/min)	Constant T. Duration (min)	Cooling method	Control parameter
Q460 [18]	20~900	Steady	15	20	Air/ Water	Elastic stage: 10MPa/s
						Yield stage: 0.001/s
						Hardening stage: 10 mm/min
S460 [19]	20~1000	Steady	10	10	Air	0.005/min
S690 [19]	20~1000	Steady	10	10	Air	0.005/min
S960 [20]	20~1000	Steady	10	10	Air	0.005/min
RQT-S690 [16]	25~800	Steady	-	10	Air	0.003/min

Table 10: Summary of post-fire tests on HSS.

Temperature range 20°C~900°C	
Air cooled	**Water cooled**
$\frac{E_T}{E} = -4\times10^{-10}T^3 + 3.93\times10^{-7}T^2 - 7.79\times10^{-5}T + 1$	$\frac{E_T}{E} = -7.15\times10^{-10}T^3 + 6.86\times10^{-7}T^2 - 9.27\times10^{-5}T + 1$
$\frac{f_{yT}}{f_y} = -1.73\times10^{-9}T^3 + 1.25\times10^{-6}T^2 - 8.05\times10^{-5}T + 1$	$\frac{f_{yT}}{f_y} = -1.73\times10^{-9}T^3 + 1.25\times10^{-6}T^2 - 8.05\times10^{-5}T + 1$
$\frac{f_{uT}}{f_u} = -3.81\times10^{-10}T^3 - 6.36\times10^{-8}T^2 + 1.79\times10^{-4}T + 1$	$\frac{f_{uT}}{f_u} = 8.11\times10^{-10}T^3 - 7.03\times10^{-7}T^2 + 1.93\times10^{-4}T + 1$
$\frac{\varepsilon_T}{\varepsilon} = 1.68\times10^{-9}T^3 - 9.55\times10^{-7}T^2 - 1.62\times10^{-4}T + 1$	$\frac{\varepsilon_T}{\varepsilon} = -1.37\times10^{-9}T^3 + 1.78\times10^{-6}T^2 - 7.62\times10^{-4}T + 1$

Table 11: Empirical equations for post-fire mechanical properties of Q460 steel.

temperatures, it gave unreliable results when the temperature was raised beyond 700°C.

Summary and Conclusions

In this paper, test results on the mechanical properties, residual stress and compressive strength of HSS under and after fire exposure are reviewed. Empirical equations that can be used to determine the elastic modulus, yield strength and tensile strength of HSS under elevated temperature and after they have been cooled down are summarized.

Based on test results on the behavior of HSS under and after high temperature exposure, the following conclusions can be drawn:

1. The mechanical properties of HSS under elevated temperature do not show appreciable decrease until the temperature reaches 300°C.
2. The blue brittleness effect is observed on lower strength HSS tested under steady-state condition from 200°C to 450°C.
3. The reduction factors for elastic modulus, yield strength and tensile strength are different for different steel grades. The recommended reduction factors in various steel design standards were obtained based on tests of mild steel and so they should not be used for the design of HHS.

Empirical equations		Simplified equations	
$\frac{E_T}{E} = -2.69\times10^{-7}T^2 + 6.55\times10^{-5}T + 0.999$	20 ≤ T ≤ 600°C	$\frac{E_T}{E} = -3.84\times10^{-10}T^3 + 1.43\times10^{-7}T^2 - 4.18\times10^{-5}T + 1$	20 ≤ T ≤ 1000°C
$\frac{E_T}{E} = 0.947 - \frac{(T-600)^{1.618}}{68.84T}$	600<T ≤ 800°C		
$\frac{E_T}{E} = -2.545\times10^{-6}T^2 + 3.856\times10^{-3}T + 0.598$	800<T ≤ 1000°C		
$\frac{f_{yT}}{f_y} = -1.19\times10^{-9}T^3 + 1.03\times10^{-6}T^2 + 2.25\times10^{-4}T + 1.004$	20 ≤ T ≤ 800°C	$\frac{f_{yT}}{f_y} = -3.24\times10^{-10}T^3 + 4.98\times10^{-8}T^2 + 4.52\times10^{-5}T + 0.998$	20 ≤ T ≤ 1000°C
$\frac{f_{yT}}{f_y} = 0.876 - \frac{(T-800)^{3.634}}{2.048\times10^6 T}$	800<T ≤ 1000°C		
$\frac{f_{uT}}{f_u} = -1.24\times10^{-9}T^3 + 1.07\times10^{-6}T^2 - 2.54\times10^{-4}T + 1.005$	20 ≤ T ≤ 750°C	$\frac{f_{uT}}{f_u} = -2.79\times10^{-7}T^2 + 1.08\times10^{-4}T + 0.996$	20 ≤ T ≤ 1000°C
$\frac{f_{uT}}{f_u} = 0.876 - \frac{(T-800)^{3.634}}{2.048\times10^6 T}$	750 < T ≤ 1000°C		

Table 12: Empirical and simplified equations for post-fire mechanical properties of S460 steel.

Empirical equations	Temperature range (°C)
$\frac{E_T}{E} = -1.52\times10^{-10}T^3 + 2.7\times10^{-8}T^2 - 3.35\times10^{-5}T + 1$	20 ≤ T ≤ 600
$\frac{E_T}{E} = 6.27\times10^{-9}T^3 - 1.38\times10^{-5}T^2 + 8.95\times10^{-3}T - 0.806$	600<T ≤ 1000
$\frac{f_{yT}}{f_y} = 1 - \frac{(T-20)^{1.584}}{9957T}$	20 ≤ T ≤ 650
$\frac{f_{yT}}{f_y} = 1.8\times10^{-8}T^3 - 4.03\times10^{-5}T^2 + 2.74\times10^{-2}T - 4.711$	650<T ≤ 1000
$\frac{f_{uT}}{f_u} = 1$	20 ≤ T ≤ 600
$\frac{f_{uT}}{f_u} = -1.24\times10^{-10}T^4 + 4.13\times10^{-7}T^3 - 5.077\times10^{-4}T^2 + 0.271T - 52.21$	600 < T ≤ 1000

Table 13: Empirical equations for post-fire mechanical properties of S690 steel.

4. The post-fire mechanical properties loss of S460, S690 and S960 are negligible for temperature below 600°C. Also, ductile failure with necking was observed during the test.
5. The type of cooling method used can affect the results, and so different empirical equations should be used for design.
6. The steel grade and alloy compositions can have a significant influence on both the during-fire and post-fire performance of HSS.
7. The residual stress distribution of HSS welded sections is similar to that of mild steel but with lower magnitudes. The residual stress magnitude of post-fire HSS welded sections tends to decrease with an increase in temperature.
8. Similar to columns made from mild steel, for a given constrained stiffness the critical temperature of HSS columns decreases when the axial load ratio increases. And for a given axial load ratio, the constrained stiffness needs to be increased to maintain the critical temperature.
9. As for the local instability behavior, the failure modes of HSS columns tested at different elevated temperatures are similar to those under room temperature. In addition, as temperature

Empirical equations	Simplified equations	Temperature range (°C)
$\frac{E_T}{E} = -1.52\times10^{-10}T^3 + 2.7\times10^{-8}T^2 - 3.35\times10^{-5}T + 1$		20 ≤ T ≤ 600
$\frac{E_T}{E} = 6.27\times10^{-9}T^3 - 1.38\times10^{-5}T^2 + 8.95\times10^{-3}T - 0.806$		600<T ≤ 1000
$\frac{f_{yT}}{f_y} = 1$	$\frac{f_{yT}}{f_y} = 1$	20 ≤ T ≤ 600
$\frac{f_{yT}}{f_y} = 8.157\times10^{-9}T^3 - 1.685\times10^{-5}T^2 + 9.388\times10^{-3}T - 0.333$	$\frac{f_{yT}}{f_y} = 4.4\times10^{-6}T^2 - 8.637\times10^{-3}T + 4.596$	600 <T ≤ 1000
$\frac{f_{uT}}{f_u} = 1$		20 ≤ T ≤ 600
$\frac{f_{uT}}{f_u} = 1.006 - \frac{(T-600)^{1.158}}{9.567\times10^5 T}$		600 < T < 800
$\frac{f_{uT}}{f_u} = 7.762\times10^{-6}T^2 - 1.568\times10^{-2}T + 8.564$		800 ≤ T ≤ 1000

Table 14: Empirical and simplified equations for post-fire mechanical properties of S960 steel.

Steel properties	Welding details	Section dimension (mm)	Heated temperatures (°C)
E=208.5 GPa f_y=538.1 MPa f_u=611.1 MPa	Fillet welds with 8 mm leg size CO_2 shielded arc welding Voltage=25V and Amps=230A Welding speed=35 cm/min Filler wire type is JM-60, with f_y=545 MPa and 25% elongation after fracture	Flame-cut 200 × 200 × 8 × 8	200/400/600/800 Natural air cooling

Table 15: Residual stress tests on post-fire HSS Welded H-sections (Wang [26,27]).

Specimen Labels	Method	Mechanical properties	Length	Section type	Section size (mm)	Axial load ratio	Axial restrained ratio (%)	Critical temp. (°C)
S1	ISO-834 Increasing temperature under constant load	8 mm Steel Plate E=212 GPa F_y=585 MPa F_u=660 MPa	4.3 m	Welded H-shaped	H300 × 150 × 6.5 × 9	0.25	9.4	620
S2						0.41	9.4	510
S3					H200 × 150× 6 × 9	0.26	3.8	625
S4						0.41	3.8	564

Table 16: Tests on Q460 H-shaped axially restrained columns for critical temperature (Wang and Ge [31]).

increases, the rate of decrease for buckling strength is faster than that for yield strength because inelastic buckling strength at elevated temperature is affected by a simultaneous reduction in yield strength and stiffness of the test specimens.

Recommendations for Further Research

Although study on the behavior of HSS at elevated temperature has been carried out by a number of researchers at both the material and structural levels, there are no standardized test methods and so the results are not always comparable. More importantly, current research on the behavior of HSS under elevated temperature is still at a stage when it is not yet ready for incorporation into steel design standards.

Research on post-fire behavior of HSS is quite limited and current standards do not contain sufficient guidelines on how the residual capacity of HSS after fire exposure can be evaluated. In addition, because the manner of how the test specimens are cooled could influence their post-fire mechanical properties, more systematic study on the post-fire mechanical properties of HSS needs to be performed and the influence of different cooling methods on the post-fire behavior of HSS needs to be considered.

For steel structures, the presence of residual stress in welded built-up members is an important design parameter to consider as it affects the inelastic behavior of the members. Due to the difference in strength between mild steel and HSS, the residual stress in HSS sections tends to be less detrimental to member strength. However, because both

Specimen labels	Steel type	Element type	Dimension (mm)	Load ratio	Slenderness ratio	Restrained ratio (%)	Critical Temperature (°C)
1	Q460	PLANE82 BEAM188 COMBINE14	Length: 3000 Section: H200x150x6x9	0.3	60	2.5	714
2				0.3	60	1.5	732
3				0.3	100	2.5	662
4				0.3	100	1.5	703
5				0.5	60	2.5	626
6				0.5	60	1.5	641
7				0.5	100	2.5	525
8				0.5	100	1.5	555
9	Q235			0.3	60	2.5	601
10				0.3	60	1.5	624
11				0.3	100	2.5	588
12				0.3	100	1.5	615
13				0.5	60	2.5	534
14				0.5	60	1.5	556
15				0.5	100	2.5	486
16				0.5	100	1.5	531

Table 17: Finite element analysis on critical temperature of axially restrained columns (Ge and Wang [32]).

Specimen labels	Temperature (°C)	Section dimension (mm)	Study objective	Test Yield strength (MPa)	Test buckling stress (MPa)
Q235A-1	25	H250 × 250 × 6 × 8	Flange local buckling	306.3	240.6
Q235A-2	450			251.6	148
Q235A-3	650			101.4	44.4
Q460A-1	25	H250 × 220 × 8 × 8		538.1	391.9
Q460A-2	450			532	278.2
Q460A-3	650			275	74.2
Q235B-1	25	H316 × 200 × 6 × 8	Web local buckling	321.9	192.6
Q235B-2	450			264.5	150
Q235B-3	650			106.6	53
Q460B-1	25	H336 × 160 × 8 × 8		538.1	356.4
Q460B-2	450			532	273.4
Q460B-3	650			275	70.3

Table 18: Stability analysis of Welded H-shaped Stub Columns under axial compression at elevated temperatures (Wang et al. [33]).

Element type	Mesh size	Boundary conditions	Column size	Analysis method
S4R5	10 mm × 10 mm	Fixed-end Pinned-end	Stub Slender	Step 1: Eigenvalue analysis (linear and elastic) Step 2: Load-displacement nonlinear analysis

Table 19: Numerical analysis of HSS Box and I-section columns at elevated temperatures (Chen and Young [34]).

the magnitudes and distributions of residual stress could undergo noticeable changes after fire, additional study beyond those reported by Wang et al. [26,27] on post-fire effect of residual stress on HSS sections needs to be carried out.

References

1. Gustafson K (2007) Steel wise Evaluation of existing structures. Modern Steel Construction pp: 3.
2. Qu L, Li H (2004) Study on strength of Q420 steel section at elevated temperature. Fire Science and Technology 5: 223-225.
3. Wang WY, Liu B, Kodur V (2012) Effect of temperature on strength and elastic modulus of high strength steel. Journal of Materials in Civil Engineering 25: 174-182.
4. Wang WY, Liu B, Li GQ (2012) Experimental study on mechanical properties of Q460 high strength steel at elevated temperature. Journal of Disaster Prevention and Mitigation Engineering 35: 30-35.
5. Mäkeläinen P, Outinen J, Kesti J (1998) Fire design model for structural steel S420M based upon transient-state tensile test results. Journal of Constructional Steel Research 48: 47-57.
6. Outinen J, Mäkeläinen P (2004) Mechanical properties of structural steel at elevated temperatures and after cooling down. Fire and Materials 28: 237-251.
7. Schneider R, Lange J (2009) Constitutive equations of structural steel S460 at high temperatures. Nordic Steel Construction Conference. Malmö, Sweden 2: 204-211.
8. Schneider R, Lange J (2012) Analysis of the time-dependent mechanical behavior of S460 in case of fire. Stahlbau 81: 379-390.
9. Schneider R, Lange J (2011) Constitutive equations and empirical creep law of steel S460 under high temperatures. Journal of Structural Fire Engineering 2: 217-230.
10. Lange J, Wohlfeil N (2010) Examination of the mechanical properties of steel S460 for fire. Journal of Structural Fire Engineering 1: 189-204.
11. Qiang X, Bijlaard FSK, Kolstein H (2012) Deterioration of mechanical properties of high strength steel S460N under steady state fire condition. Materials & Design 36: 438-442.
12. Qiang X, Bijlaard FSK, Kolstein H (2012) Deterioration of mechanical properties of high strength steel S460N under transient state fire condition. Materials & Design 40: 521-527.
13. Qiang X, Bijlaard FSK, Kolstein H (2012) Elevated-temperature mechanical properties of high strength structural steel S460N: Experimental study and recommendations for fire-resistance design. Fire Safety Journal 55: 15-21.
14. Chen J, Young B, Uy B (2006) Behavior of high strength structural steel at elevated temperatures [J]. Journal of Structural Engineering 132: 1948-1954.
15. Qiang X, Bijlaard FSK, Kolstein H (2012) Dependence of mechanical

properties of high strength steel S690 on elevated temperatures. Construction and Building Materials 30: 73-79.

16. Chiew SP, Zhao MS, Lee CK (2014) Mechanical properties of heat-treated high strength steel under fire/post-fire conditions. Journal of Constructional Steel Research 98: 12-19.
17. Li GQ, Jiang SC, Yin YZ, Chen K, Li MF (2003) Experimental studies on the properties of constructional steel at elevated temperatures. Journal of Structural Engineering 129: 1717-172.
18. Wang WY, Liu T, Liu J (2015) Experimental study on post-fire mechanical properties of high strength Q460 steel. Journal of Constructional Steel Research 114: 100-109.
19. Qiang X, Bijlaard FSK, Kolstein H (2012) Post-fire mechanical properties of high strength structural steels S460 and S690. Engineering Structures 35: 1-10.
20. Qiang X, Bijlaard FSK, Kolstein H (2013) Post-fire performance of very high strength steel S960. Engineering Structures 80: 235-242.
21. Wang YB, Li GQ, Chen SW (2012) Residual stresses in welded flame-cut high strength steel H-sections. Journal of Constructional Steel Research 79: 159-165.
22. Ban H, Shi G, Bai Y (2013) Residual stress of 460MPa high strength steel welded I section: experimental investigation and modeling. International Journal of Steel Structures 13: 691-705.
23. Yang B, Nie S, Xiong G (2016) Residual stresses in welded I-shaped sections fabricated from Q460GJ structural steel plates. Journal of Constructional Steel Research 122: 261-273.
24. Kim DK, Lee CH, Han KH (2014) Strength and residual stress evaluation of stub columns fabricated from 800MPa high-strength steel. Journal of Constructional Steel Research 102: 111-120.
25. Li TJ, Li GQ, Wang YB (2015) Residual stress tests of welded Q690 high-strength steel box- and H-sections. Journal of Constructional Steel Research 115: 283-289.
26. Wang WY, Li GQ, Ge Y (2015) Residual stress study on welded section of high strength Q460 steel after fire exposure. Advanced Steel Construction 11: 150-164.
27. Wang WY, Li GQ, Ge Y (2016) Experimental investigation of residual stresses in thin-walled welded H-sections after fire exposure. Thin-Walled Structures 101: 109-119.
28. Valente JC, Neves IC (1999) Fire resistance of steel columns with elastically restrained axial elongation and bending. Journal of Constructional Steel Research 52: 319-333.
29. Rodrigues JPC, Neves IC, Valente JC (2000) Experimental research on the critical temperature of compressed steel elements with restrained thermal elongation. Fire Journal 35(2): 77-98.
30. Tan KH, Toh WS, Huang ZF, Phng GH (2007) Structural responses of restrained steel columns at elevated temperatures. Part 1- Experiments. Engineering Structures 29: 1641-1652.
31. Wang WY, Ge Y (2012) Experimental study on fire resistance of axially restrained high strength Q460 steel columns. Journal of Building Structures 36: 116-122.
32. Ge Y, Wang WY (2012) Fire resistance analysis of restrained high strength steel Q460 columns. Journal of Disaster Prevent and Mitigation Engineering 32: 99-104.
33. Wang WY, Yang XC, Wang B, Mu HL (2014) Experimental study on local stability of welded H-shaped steel stub columns under axial compression at elevated temperature. Journal of Building Structures 35: 134-142.
34. Chen J, Young B (2008) Design of high strength steel columns at elevated temperatures. Journal of Constructional Steel Research 64: 689-703.